Int. J. Electrochem. Sci., 10 **(2015)** 223 - 234

International Journal of
ELECTROCHEMICAL
SCIENCE
www.electrochemsci.org

Electrochemical Study of Metribuzin Pesticide Degradation on Bismuth Electrode in Aqueous Solution

Bogdan Tutunaru, Adriana Samide, Anca Moanţă, Cătălina Ionescu, Cristian Tigae[*]

University of Craiova, Faculty of Mathematics and Natural Sciences, Department of Chemistry, Calea Bucureşti 107i, Craiova, România
[*]E-mail: ctigae@yahoo.com;

Received: 18 September 2014 / *Accepted:* 29 October 2014 / *Published:* 17 November 2014

To discuss the metribuzin pesticide (MBZ) stability, in order to prevent the environmental pollution, its electrochemical behaviour on bismuth electrode was studied by cyclic voltammetry (CV), electrochemical impedance spectroscopy (EIS) and current constant electrolysis associated with UV-Vis spectrophotometry. The contribution of both Cl^- as well as NO_3^- ions on metribuzin electrochemical behaviour was studied, indicating that the pesticide was degraded in ratio of 89.3 % in the absence of chloride ions and 47.5 % in their presence. Moreover, the degradation mechanism of metribuzin was proposed.

Keywords: metribuzin pesticide; electrochemical degradation; bismuth electrode.

1. INTRODUCTION

The mercury was reported as suitable electrode for electrochemical degradation of organic compounds because of its renewable surface and cathodic potential window. However, due to the toxicity, the mercury electrode was replaced with other electrodes such us: boron-doped diamond, bismuth and antimony [1-5].

The bismuth electrodes have an electrochemical behaviour similar to ideally polarizable electrodes [6]. These were characterized by cyclic voltammetry and electrochemical impedance spectroscopy associated with [7] the scanning electron microscopy, concluding that the electrochemical activity of porous surface is lower than the one of smooth surface. The electrochemical investigation of bismuth electrodes in different media showed that the film containing Bi_2O_3 and BiOOH [8, 9] was formed on the substrate surface. The bismuth electrode was used for voltammetric study of 2-amino-6-nitrobenzothiazole (genotoxic and mutagenic dye), in the concentration range from 0.2 to 10 μmol L^{-1}, at pH = 7 [10]. α-Glucosidase was immobilized on glassy

carbon electrode modified with bismuth film, in order to analyze two inhibitors of this enzyme [11]. The drugs such as: aminosalicylate [12], sulfadiazine [13] and sildenafil [14] were investgated by cyclic voltammetry on bismuth electrode. Also, these electrodes have been employed for electrochemical determination of many metal ions [15-17]. The electrodes made from antimony were also characterized [18-20], in order to investigate the electrochemical behaviour of different pollutants [21-24].

The intensive utilization of pesticides as a strategy to improve agricultural productivity induces environmental and toxicological risks, groundwater contamination and serious health problem to the population. In the last decade, several techniques have been employed for treatement of waters polluted with pesticides [25-27]. The electroreduction of different pesticides on dropped mercury electrode indicates the presence of some complicated phenomena related to acid-base equilibrium [28].

Electrochemical reduction of metribuzin herbicide was studied on different electrodes (glassy carbon, carbon paste, activated granular carbon, mercury drop, poly(o-ethoxyaniline)) and by different methods (anodic stripping voltammetry, electrosorption, photocatalytic degradation and ultraviolet oxidation) [29-42]**.** Photodecomposition on the soil surface and in aqueous media was also an important process in the degradation of metribuzin and showed that the increase in soil organic matter enhanced degradation [43-45]. Optimal metribuzin biodegradation by a highly efficient metribuzin degrading bacterium, *Bacillus* sp. N1 occurred at a temperature of 30ºC and at pH 7.0 [46].

In the present study, the electrochemical behaviour of metribuzin pesticide (MBZ), IUPAC name: 4-amino-6-(1,1-dimethylthio-3-(methylthio)1,2,4-triazin-5(4H)-one was investigated. The cyclic voltammetry and electrochemical impedance spectroscopy (EIS) were performed on bismuth electrode in solutions containing Cl^- and NO_3^- ions, in the absence and in the presence of MBZ, in order to obtain the information related to pesticide stability to prevent environmental pollution.

2. EXPERIMENTAL

2.1 Materials

In all electrochemical experiments, working and auxiliary electrodes were made from pure bismuth (active area of 2.0 cm^2, Merck provenience, p.a. 99.999 %). Electrolyte solutions with the following compositions: 1) 10^{-1} M $NaNO_3$; 2) 10^{-1} M $NaNO_3$, 10^{-4} M MBZ; 3) 10^{-1} M $NaNO_3$, 10^{-1} M NaCl; 4) 10^{-1} M $NaNO_3$, 10^{-1} M NaCl, 10^{-4} M MBZ, were used to perform the cyclic voltammetry and EIS measurements on bismuth electrode. All chemicals with analytical reagent grade were obtained from Merck, being used without further purification. The molecular structure of MBZ is shown in Fig. 1.

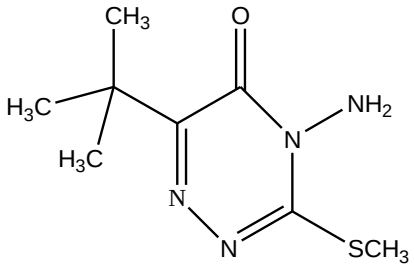

Figure 1. The molecular structure of MBZ.

2.2 Methods and techniques

2.2.1 Cyclic voltammetry

Cyclic voltammetric experiments, at a scan rate of 10 mV s^{-1} were registered for ten successive cycles in the potential range of -1.5 ÷ +1.0 V on bismuth electrode in electrolyte solutions above mentioned, in order to differentiate the influence of NO_3^- and Cl^- ions on MBZ electrochemical behaviour.

2.2.2 Electrochemical impedance spectroscopy

The electrochemical impedance spectra, corresponding to bismuth electrode were recorded in the same solutions above described, after the bismuth immersion time of 4.0 minutes, at open circuit and room temperature, in the frequency range of 100 kHz - 10 mHz, with the ac voltage amplitude of 10 mV. Both, cyclic voltammetry as well as the EIS experiments were performed using a VoltaLab 40 potentiostat/galvanostat with VoltaMaster 4 software. A standard electrochemical cell with three electrodes was used. The working and auxiliary electrodes were represented by pure bismuth. All potential values are reported with respect to reference $Ag/AgCl_{sat.}$ electrode. Before of each experiment, the working and auxiliary electrodes were polished with emery paper, washed with distilled water, degreased with ethanol and dried in warm air. All experiments were carried out at room temperature of 23 ± 1 °C.

2.2.3 UV-Vis spectrophotometry

The electrochemical degradation of MBZ aqueous solutions (each of 100 mL) in the presence of NO_3^-, without and with Cl^- ions was performed with a Keithley 2420 3A SourceMeter potentiostat/galvanostat, in dynamic conditions using a magnetic stirrer (stirring rate of 300 rpm), under constant current of 200 mA (current density 50 mA cm^{-2}), electrolysis time being of 1.0 hour. The electrochemical degradation of MBZ was investigation by the monitoring of absorbance values at different times: 10 min.; 20 min.; 40 min.; 60 min, using an UV-Vis Varian Cary 40 spectrophotometer, with CaryWin UV software, at wavelength range between 500 and 200 nm. The

maximum absorbance values at 295 nm (λ_{max}) were used to calculate de percentage degradation degree (*DG* %) of MBZ.

2.2.4 Surfaces morphology

The surface morphology of bismuth electrode, before and after electrochemical degradation of metribuzin, was examined by Euromex microscope, with Canon camera and included ZoomBrowser - EOS Digital software.

3. RESULTS AND DISCUSSION

3.1 Cyclic voltammetry

The Figure 2 illustrates the first and tenth cycle of cyclic voltammetry obtained for bismuth electrode in 10^{-1} M NO_3^- blank solution and in 10^{-1} M NO_3^- solution containing 10^{-4} M MBZ, in potential range between -1.5 and + 1.2 V.

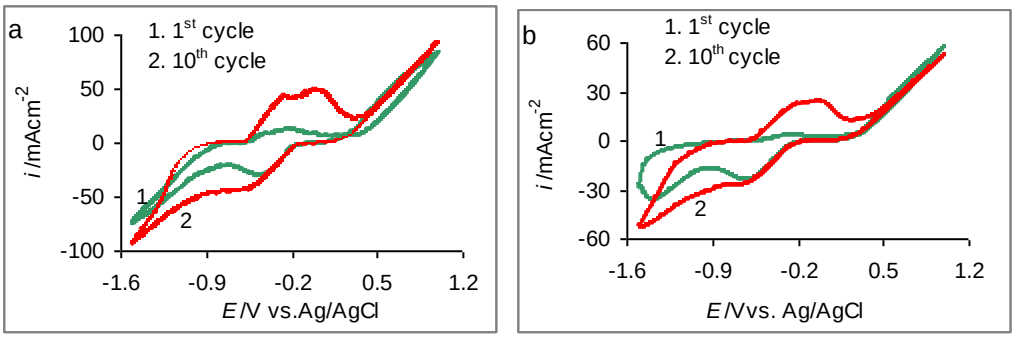

Figure 2. Cyclic voltammograms of bismuth electrode obtained in: a - 10^{-1} M $NaNO_3$ solution in the absence of MBZ; b - in the presence of 10^{-4} M MBZ.

In the absence of MBZ (Fig. 2a) two anodic peaks are observed corresponding to -0.25 and 0.0 V which can be associated with bismuth oxidation to produce the growth of a Bi_2O_3 film [47]. In the presence of MBZ, all current densities (anodic and cathodic) were reduced at half, indicating that the pesticide acts *via* adsorption of its molecules on metal surface (Fig. 2b).

For both solutions without and with MBZ (Figs. 2a and 2b), the cathodic peak obtained at -0.5 V, during the negative scan, is attributed to the electrochemical reduction of Bi_2O_3 film that was formed during the positive scan [47]. Thus, at potentials more negative than -1.0 V, the increase of cathodic current densities is attributed to the hydrogen evolution reaction. The addition of MBZ leads to occurrence of a new cathodic peak at -1.4 V, corresponding to the reduction of the azomethine bond from MBZ structure, this being overlapped on the hydrogen evolution reaction [31].

By the addition of Cl^- ions (Fig. 3) in both solutions above mentioned the second anodic peak at 0.0 V is observed only on the first cycle. During the scan of the tenth cycle was recorded a new peak at higher anode potential of 0.7 V, and that could correspond to the formation of oxy/chlorinated

species of bismuth (Fig. 3a). At higher anodic potential, Bi_2O_3 becomes thermodynamically unstable, this being converted in BiOCl. Consequently, the oxide can exist as a metastable phase, because a low rate of mass transfer of chloride ions in the film takes place. The increase of potential values leads to the change of film properties due to the formation of a new salt as $Bi(OH)Cl_2$, with a lower basicity compared to that of BiOCl [48]. The presence of chloride ions changes the composition and also, the structure of oxide film formed on the electrode surface during the anodic polarization, consequently, both shapes of anodic and cathodic polarization curves are modified. Moreover, the second cathodic peak (-0.8 V) was recorded and this could be attributed to the reduction of chlorinated species of bismuth (Fig. 3a).

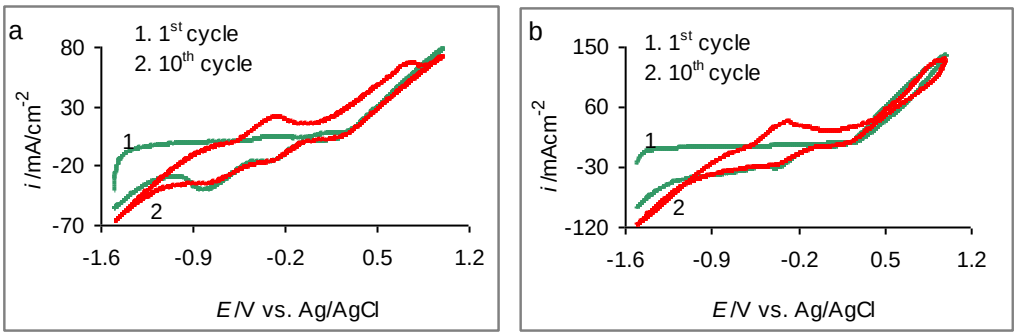

Figure 3. Cyclic voltammograms of bismuth electrode obtained in the solutions containing: a - 10^{-1} M $NaNO_3$ and 10^{-1} M NaCl in the absence of MBZ ; b - 10^{-1} M $NaNO_3$ and 10^{-1} M NaCl in the presence of 10^{-4} M MBZ.

The addition of MBZ to electrolyte solution (Fig. 3b), both peaks, at anodic value of 0.7 V, as well as the cathodic peak recorded at -0.8 V are less nuanced. These two peaks are attributed to the formation (0.7 V) and the reduction (-0.8 V) of oxy/chlorinated compounds of bismuth, meaning that the MBZ could favour electrode dissolution, and consequently the synergistic effect on electrochemical processes between chloride ions and MBZ molecules being a truthful assumption.

Based on these above mentioned, it can be concluded that: (i) MBZ protects the electrode surface, the current densities having lower values (Fig. 2b) than those were recorded in its absence (Fig. 2a); (ii) the presence of chloride ions leads to the formation of new oxy/chlorinated compounds on electrode surface, only in the absence of metribuzin (Fig. 3a); (iii) in the presence of both chloride ions and MBZ, the formation and reduction of oxy/chloride species is not so obvious. These species are relatively unstable, interacting more easily with the MBZ, and favouring faster electrode dissolution which is in full agreement with the current density values recorded in this case. (Fig. 3b).

3.2 Electrochemical impedance spectroscopy

To obtain more information about occurred processes at the electrode/solution interface, EIS measurements of bismuth electrode in the same media above mentioned were performed. Their results are illustrated in Fig. 4. In the absence of chloride ions (Fig. 4a) the Nyquist diagram was obtained, in both cases, in the absence and in the presence of MBZ, the impedance plot being characterized by two

distinct regions: (i) a semicircle at high frequency region related to charge transfer process, that is more nuanced in the absence of MBZ; (ii) a line, at low frequencies region where the plots define the diffusion of species on the electrode surface. Thus, in the absence of MBZ the capacitive loop occurred at high frequency indicates the formation of Bi_2O_3 layer that is less obvious in the presence of organic molecules indicating that MBZ inhibits the Bi oxidation.

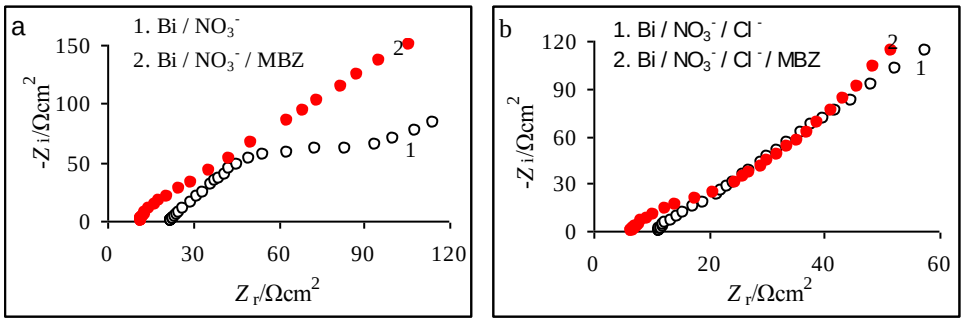

Figure 4. Nyquist diagrams of bismuth electrode obtained in: a - 10^{-1} M $NaNO_3$ solution in the absence and in the presence of 10^{-4} M MBZ; b - the solutions containing 10^{-1} M $NaNO_3$ and 10^{-1} M NaCl without and with 10^{-4} M MBZ.

In the presence of chloride ions (Fig. 4b) similar Nyquist spectra were obtained for the solution without and with MBZ. At high frequency region, in the presence of MBZ a more pronounced capacitive loop was recorded indicating that the MBZ molecules activate bismuth dissolution. The enrichment of the oxidic coating with chloride ions in a region close to the substrate/electrolyte interface can be interpreted in terms as a developing of partially homogenous layer characterized by a different dielectric constant [8]. This behaviour demonstrates that the electrode reaction is controlled by charge transfer and diffusion processes [9].

Consequently, the results obtained from EIS measurements are in good agreement with those were provided by cyclic voltammetry.

3.3 UV-Vis spectrophotometry

Further evidences of electrochemical behaviour of MBZ were provided by UV-Vis spectrophotometry. UV-Vis spectra of aqueous solutions containing 10^{-1} M $NaNO_3$, 10^{-4} M MBZ and 10^{-1} M $NaNO_3$, 10^{-1} M NaCl, 10^{-4} M MBZ were recorded at different times: 10 min.; 20 min.; 40 min.; 60 min., at wavelengths between 200-500 nm (Fig. 5).

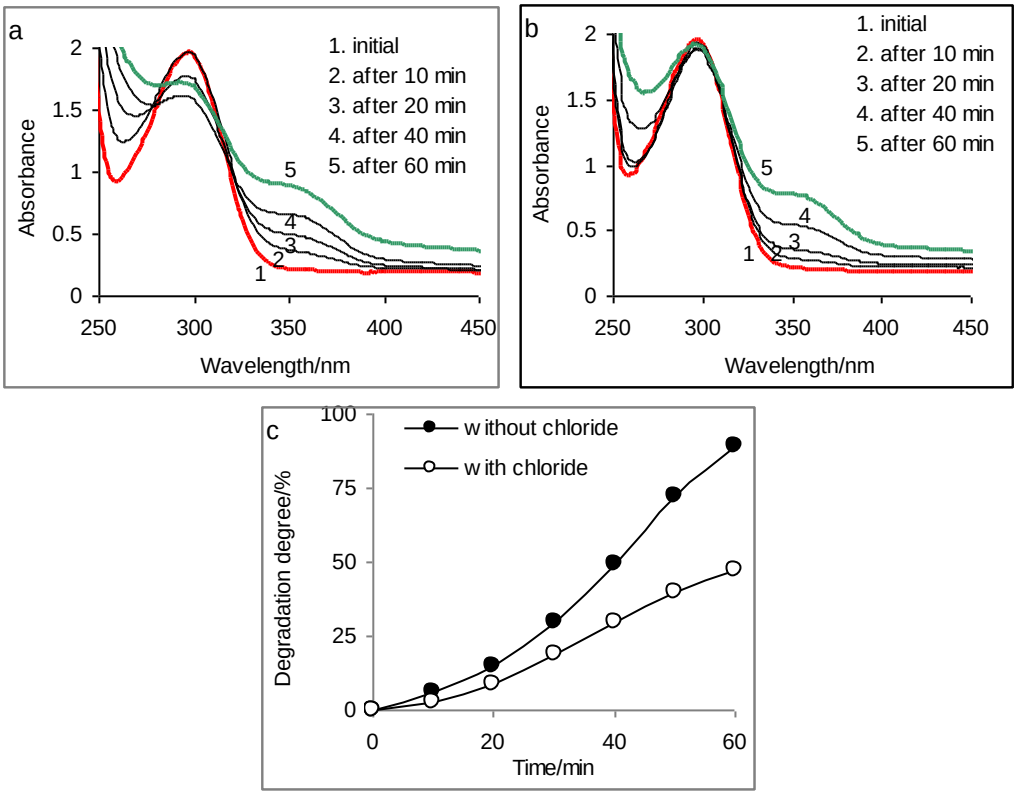

Figure 5. Degradation degree of MBZ and UV-Vis spectra of the solution containing: a - 10^{-1} M $NaNO_3$ and 10^{-4} M MBZ; b - 10^{-1} M $NaNO_3$; 10^{-1} M NaCl; 10^{-4} M MBZ; c - degradation degree of MBZ evaluated in both solutions above mentioned.

It has been demonstrated that the film formation on bismuth electrode is suitable for cathodic degradation of different organic compounds such as: pesticide or drugs [13]. This presents the great advantage because it is not sensitive to the presence of dissolved oxygen [49]. The modified bismuth film on glassy carbon (BiF-GCE) and the modified bismuth bulk mixed with carbon paste, were applied for the determination of nitroguanidine and neonicotinoide insecticides [49]. The bismuth film (BiFE) prepared ex-situ on a support of glassy carbon electrode was efficient to investigate the electrochemical behaviour of aminosalycilate drugs (sulfasalazine and olsalazine sodium) [50]. The results indicated that the BiFE improves the sensitivity related to electrochemical reduction of these drugs. Also, some studies have been reported the amperometric and voltametric detections of 2-nitrophenol and bromofenoxim on bismuth electrode [51, 52]. Daunomycin and picric acid have been reported as electrochemical indicators which can form self-assembled monolayers (SAMs) on bismuth bulk electrodes (BiBEs) [53].

In the absence of chloride ions (Fig. 5a), the maximum of MBZ absorption around 295 nm shifts to smaller absorbance values, consequently the MBZ concentration follows the same trend. This can induce the idea that the MBZ molecules can be adsorbed on the electrode surface or these can interact with the bismuth atoms and/or with oxidized active species from the metal surface. The increase of adsorption maximum, at wavelength of 348 nm, can be attributed to the new compound formed in solution. The degradation mechanism of MBZ was proposed, as shown in Scheme 1.

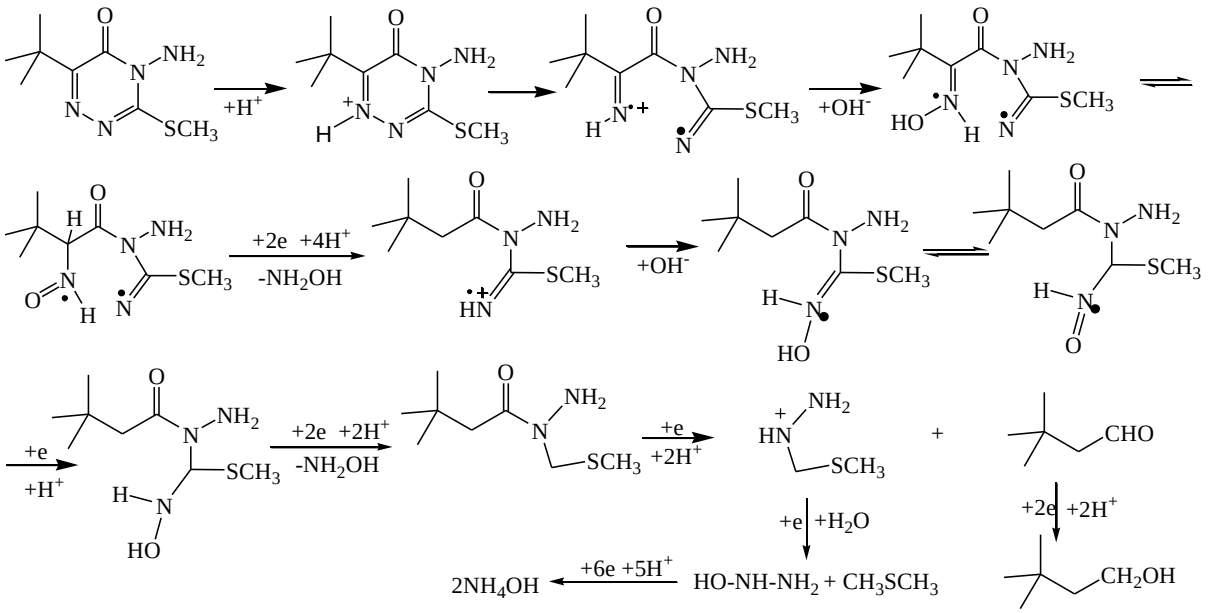

Scheme 1. The degradation mechanism of MBZ

The molecule of metribuzin herbicide is quite complex, this containing four nitrogen atoms with the oxidation state of -2, thus in the presence of protons it may participate in reduction reactions. The nitrogen atoms from triazinone ring are the most susceptible to reduction reaction. The first step of metribuzin degradation is represented by the protonation of azomethine bond before electron transfer processes [12]. The first attack of protons is in positions 1 or 2 of triazinone cycle [54].

Reduction of both azomethine bonds (1-6 and 2-3) is accompanied by acid-base equilibria and hydration-dehydration process. The nitrogen atom may be removed sequentially as hydroxylamine or ammonium hydroxide. The byproducts such as: dimethyl thioether and 3,3-dimethyl-1-butanol show the maximum reduction state and these can not participate in the subsequent reduction reactions.

In the presence of chloride ions, after 1.0 hour the same absorbance value at wavelength of 295 nm (Fig. 5b) was recorded, but the gradually shifting of baseline indicates the decrease of MBZ concentration and the increase of adsorption maximum observed at 348 nm. This absorption band is attributed to degradation and/or coordination products of MBZ. In the absence of chloride ions, the adsorption and/or degradation of MBZ prevails the oxidation of the bismuth electrode, while the presence of chloride ions favors the dissolution of the latter. The best way to express quantitatively those early mentioned is to calculate the degradation degree (*DG*) of MBZ in the both cases using the following equation, Eq. 1.

$$DG\ \% = (1- A_t/A_o)\cdot 100 \qquad (1)$$

where A_o and A_t represents the initial absorbance value and the absorbance value at time "t".

As shown the Fig. 5c in the absence of chloride ions *DG* reaches a maximum value of 89.3 %, while the presence of chloride ions leads to a smaller MBZ degradation degree reaching a value of 47.5 % after 1.0 h of electrolysis, attesting that the parallel courses of MBZ degradation and electrode

dissolution may occur. These results confirm all information provided by cyclic voltammetry and EIS measurements.

3.4 Surfaces morphology

The surface morphologies of bismuth electrode, before and after electrochemical degradation of metribuzin, were analyzed by metallographic microscope Euromex type (Fig. 6).

The structured area obtained after anodic polarization (Fig. 6b) is not characteristic of a cleaved bismuth surface, but rather of a chemically or electrochemically etched Bi surface. Electrochemical reactions lead to the bismuth dissolution that occurs preferably at the surface defects of the Bi electrode, resulting in the formation of stepped Bi surface like demonstrated in Fig. 6b.

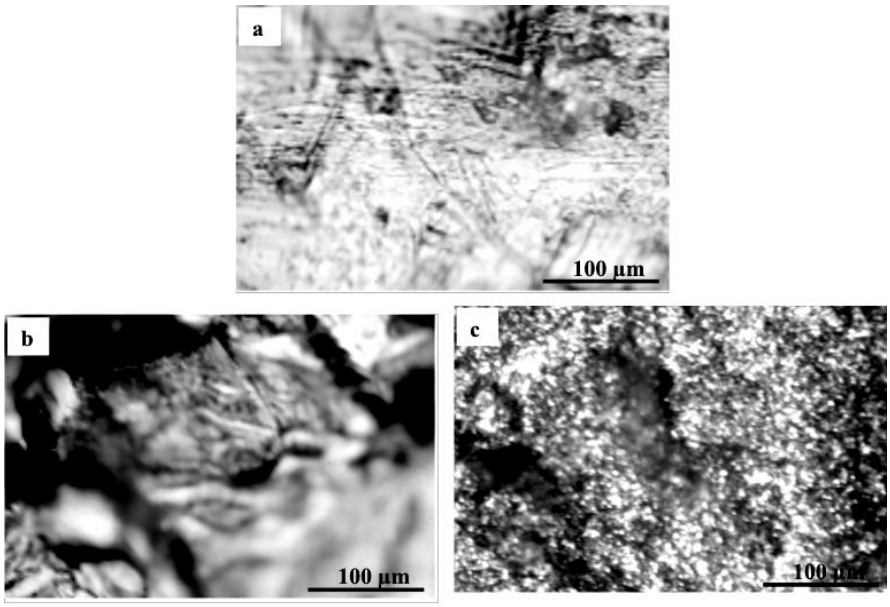

Figure 6. Surface morphology of bismuth electrodes: before anodic polarization (a); after anodic (b) and cathodic (c) polarization.

The magnitude of *i* vs. *E*-curves in Figs. 2 and 3 also demonstrates a noticeable roughening of the Bi electrode surface during holding it at i = 50 mA/cm^2. Micrograph images of the resulting surfaces after catodic polarization (Fig. 6c) indicate the presence of the porous Bi layers on smooth Bi surface. The black spots are most likely the pores. Similar micrographs of bismuth electrode surface were obtained in 0.1 M $LiClO_4$ aqueous solution [7, 55]. To establish the mechanism of anodic oxidation and cathodic reduction of bismuth electrode, in sulfuric acid solution, some techniques were used such as: SEM, XRD and EIS. Consequently, anodized electrode at the potential value close to the open-circuit value, the characteristic diffraction peaks of bismuth crystals become sharper, but with the potential increase, the feature of amorphous phase was highlighted [9].

4. CONCLUSIONS

Cyclic voltammograms of bismuth electrode obtained in 10^{-1} M $NaNO_3$ solution, in the absence and in the presence of 10^{-4} M MBZ showed that, the current densities reached lower values in the MBZ presence compared to those were recorded in its absence, indicating that, this pesticide protects the electrode surface. The presence of chloride ions leads to the formation of new oxy/chlorinated compounds on electrode surface, only in the absence of MBZ. In the presence of both: chloride ions and MBZ, the formation and reduction of oxy/chloride species is not so obvious.

EIS measurements of bismuth electrode in the same media above mentioned, as shown Nyquist, the impedance plot is characterized by two distinct regions: a semicircle at high frequency region related to charge transfer process, this being more nuanced in the absence of MBZ; a line, at low frequencies region where the plots indicating the diffusion process. In the absence of MBZ the capacitive loop at high frequency indicates the formation of Bi_2O_3 layer. In the presence of organic molecules this is less obvious, indicating that MBZ inhibits the bismuth oxidation. In the presence of chloride ions similar Nyquist spectra were obtained. At high frequency region, in the presence of MBZ a more pronounced capacitive loop was recorded indicating that, the MBZ molecules activate bismuth dissolution. Consequently, the results obtained from EIS measurements are in good agreement with those were provided by cyclic voltammetry.

UV-Vis spectrophotometry indicates that in the absence of chloride ions degradation degree reaches a maximum value of 89.3 %, while in their presence the degradation degree of MBZ reaches a smaller value of 47.5 %, after 1.0 h of electrolysis.

The degradation mechanism of MBZ was proposed. The byproducts such as: dimethyl thioether and 3,3-dimethyl-1-butanol show the maximum reduction state. These can not participate in the subsequent reduction reactions.

ACKNOWLEDGEMENTS

This work was partially supported by the grant number 39C/27.01.2014 /2014, awarded in the internal grant competition of the University of Craiova.

References

1. K. Peckova and J. Barek, *Curr. Org. Chem.*, 15 (2011) 3014.
2. A. Danhel and J. Barek, *Curr. Org. Chem.*, 15 (2011) 2957.
3. J. Tvrdikova, A. Danhel, J. Barek and V. Vyskocil, *Electrochim. Acta*, 73 (2012) 23.
4. V. Vyskocil, T. Navratil, A. Danhel, J. Dedik, Z. Krejcova, L. Skvorova, J. Tvrdikova and J. Barek, *Electroanal.*, 23 (2011) 129.
5. E.A. Hutton, B. Ogorevc and M.R. Smyth, *Electroanal.*, 16 (2004) 1616.
6. T. Romann, V. Grozovski and E. Lust, *Electrochem. Commun.*, 9 (2007) 2507.
7. T. Romann and E. Lust, *Electrochim. Acta.*, 55 (2010) 5746.
8. M.A. Perez, O.E. Linarez Perez and M. Lopez Teijelo, *J. Electroanal. Chem.*, 596 (2006) 149.
9. W.S. Li, X.M. Long, J.H. Yan, J.M. Nan, H.Y. Chen and Y.M. Wu, *J. Power Sources*, 158 (2006) 1096.
10. D. Deylova, V. Vyskocil, J. Barek and A. Economou, *Talanta*, 102 (2012) 68.
11. S. Timur and U. Anik, *Anal. Chim. Acta.*, 598 (2007) 143.

12. B. Nigovic, B. Simunic and S. Hocevar, *Electrochim. Acta.*, 54 (2009) 5678.
13. I. Campestrini, O.C. de Braga, I.C. Vieira and A. Spinelli, *Electrochim. Acta.*, 55 (2010) 4970.
14. H. Sopha, S.B. Hocevara, B. Pihlarb and B. Ogorevc, *Electrochim. Acta.*, 60 (2012) 274.
15. M. Yang, Z. Zhang, Z. Hub and J. Li, *Talanta*, 69 (2006) 1162.
16. E.A. Hutton, S.B. Hocevar, L. Mauko and B. Ogorevc, *Anal. Chim. Acta.*, 580 (2006) 244.
17. S. Legeai, S. Bois and O. Vittori, *J. Electroanal. Chem.*, 591 (2006) 93.
18. O.P. Linarez Perez, M.D. Sanchez and M. Lopez Teijelo, *J. Electroanal. Chem.*, 645 (2010) 143.
19. M. Metikos-Hukovic, R. Babic and S. Brinic, *J. Power Sources.*, 157 (2006) 563.
20. E. Svobodova-Tesarova, L. Baldrianova, M. Stoces, I. Svancara, K. Vytras, S.B. Hocevar and B. Ogorevc, *Electrochim. Acta.*, 56 (2011) 6673.
21. Ch. Comninellis, *Electrochim. Acta.*, 39 (1994) 1857.
22. X. Chen, P. Yao, D. Wang and X. Wu, *Chem. Eng. J.*, 147 (2009) 412.
23. Y.H. Song, G. Wei and R.C. Xiong, *Electrochim. Acta.*, 52 (2007) 7022.
24. J.T. Kong, S.Y. Shi, L.C. Kong, X.P. Zhu and J.R. Ni, *Electrochim. Acta.*, 53 (2007) 2048.
25. M. Lapertot, S. Ebrahimi, S. Dazio, A. Rubinelli and C. Pulgarin, *J. Photochem. Photobiol. A: Chem.*, 186 (2007) 34.
26. Z. Jia, Y. Li, S. Lu, H. Peng, J. Ge and S. Chen, *J. Hazard. Mater.*, 129 (2006) 234.
27. N. Daneshvar, S. Aber, A. Khani and A.R. Khataee, *J. Hazard. Mater.*, 144 (2007) 47.
28. P. Zuman, M. Privman, M. Shibata and J. Ludvik, *Turk. J. Chem.*, 24 (2000) 311.
29. J. Skopalova and T. Navratil, *Chem. Anal. (Warsaw)*, 52 (2007) 961.
30. O. Kitous, A. Cheikh, H. Lounici, H. Grib, A. Pauss and N. Mameri, *J. Hazard. Mater.*, 161 (2009) 1035.
31. A.C. de Andrade Lima, E.G. da Silva, M.O.F. Goulart, J. Tonholo, T.T. da Silva, F.C. de Abreu, *J. Braz. Chem. Soc.*, 20 (2009) 1698.
32. S.G. Chopade, A. Kuljarni and K. Kulakarni, *Internat. J. Chem. Sci. Technol.*, 2 (2012) 20.
33. S.A. Abdel-Gawad, A.M. Baraka, K.A. Omran and M.M. Mokhtar, *Int. J. Electrochem. Sci.*, 7 (2012) 6654.
34. H.C. Yatmaz and Y. Uzman, *Int. J. Electrochem. Sci.*, 4 (2009) 614.
35. G.G. Bessegato, V.P. Santos and C.A. Lindino, *Quim. Nova*, 35 (2012) 332.
36. O. Yahiaoui, L. Aizel, H. Lounici, N. Drouiche, M.F.A. Goosen, A. Pauss and N. Mameri, *Desalination*, 270 (2011) 84.
37. N. Priyantha and S. Weliwegamage, *Int. J. Electrochem. Sci.*, 3 (2008) 125.
38. O. Kitous, H. Hamadou, H. Lounici, N. Drouiche and N. Mameri, *Chem. Eng. Process.*, 55 (2012) 20.
39. A. Medjdoub, S.A. Merzouk, H. Merzouk, F.Z. Chiali and M. Narce, *Pest. Biochem. Physiol.*, 101 (2011) 27.
40. S.A. Alves, T.C.R. Ferreira and M.R.V. Lanza, *Quim. Nova*, 35 (2012) 1981.
41. M. Errami, R. Salghi, A. Zarrouk, A. Chakir, S. S. Al-Deyab, B. Hammouti, L.Bazzi and H. Zarrok, *Int. J. Electrochem. Sci.*, 7 (2012) 4272.
42. H. Bouya, M. Errami, R. Salghi, Lh. Bazzi, A. Zarrouk, S.S. Al-Deyab, B. Hammouti, L. Bazzi and A.Chakir, *Int. J. Electrochem. Sci.*, 7 (2012) 3453.
43. R. Khoury, C.M. Coste and N.S. Kawar, *J. Environ. Sci. Health, Part B*, 41 (2006) 795.
44. J. Kumar, K. Nisar, N.A. Shakil, S. Walia and R. Parsad, *J. Environ. Sci. Health, Part B*, 45 (2010) 330.
45. N. Singh, Raunaq, S.B. Singh, *J. Environ. Sci. Health, Part B*, 48 (2013) 587.
46. H. Zhang, Y. Zhang, Z. Hou, X. Wu, H. Gao, F. Sun and H. Pan, *J. Environ. Sci. Health, Part B*, 49 (2014) 79.
47. D.E. Williams, *Electrochim. Acta*, 21 (1976) 1097.
48. V.V. Ekilik, E.A. Korsakova, A.G. Berezhnaya and E.I. Momotova, *Prot. Met. Phys. Chem. Surf.*, 49 (2013) 826.

49. V. Guzsvany, Z. Papp, J. Zbiljic, O. Vajdle and M. Rodic, *Molecules*, 16 (2011) 4451.
50. B. Nigovic, B. Simunic and S. Hocevar, *Electrochim. Acta*, 54 (2009) 5678.
51. E.A. Hutton, B. Ogorevc, S.B. Ho eevar, F. Weldon, M.R. Smyth and J. Wang, *Electrochem. Commun.*, 3 (2001) 707.
52. R. Pauliukaite, S.B. Hocevar, B. Ogorevc and J. Wang, *Electroanal.*, 16 (2004) 719.
53. M. Adamovski, A. Zajac, P. Grundler and G.U. Flechsig, *Electrochem. Commun.*, 8 (2006) 932.
54. J. Ludvik, F. Riedl, F. Liska, P. Zuman, *Electroanal.*, 10 (1998) 869.
55. D.W. Song, W.N. Shen, B. Dunn, C.D. Moore, M.S. Goorsky, T. Radetic, R. Gronsky and G. Chen, *Appl. Phys. Lett.*, 84 (2004) 1883.